On Learning Where To Look

Marc'Aurelio Ranzato

Google Inc.* Mountain View CA, U.S.A.

Abstract

Current automatic vision systems face two major challenges: scalability and extreme variability of appearance. First, the computational time required to process an image typically scales linearly with the number of pixels in the image, therefore limiting the resolution of input images to thumbnail size. Second, variability in appearance and pose of the objects constitute a major hurdle for robust recognition and detection. In this work, we propose a model that makes baby steps towards addressing these challenges. We describe a learning based method that recognizes objects through a series of glimpses. This system performs an amount of computation that scales with the complexity of the input rather than its number of pixels. Moreover, the proposed method is potentially more robust to changes in appearance since its parameters are learned in a data driven manner. Preliminary experiments on a handwritten dataset of digits demonstrate the computational advantages of this approach.

1 Introduction

There are about 40 types of vision systems in nature [1]. Each such vision system is highly optimized for certain physical constraints, for the environment where the animal lives and for the task that it has to accomplish in order to survive. Machine vision has made many strides in the past decades with successful applications in several domains. However when compared to human vision, artificial visual systems are rather primitive in terms of their efficiency and ability to work in unrestricted domains. We conjecture that if we aim at building an artificial system that is good at tasks for which humans are good, then it may be helpful to take inspiration from some of the principles underlying the human visual system.

One striking difference between machine vision and human vision is how we process the visual world. The human visual system is foveated, meaning that its acuity (related to the density of cones in the retina) is much larger around the fovea than other areas. Moreover, humans analyze the visual world through a sequence of saccades. By integrating information across the whole sequence of glimpses, humans form a mental description of the visual world surrounding them.

Machine vision is currently more similar to the visual system of a bee instead. Eyes do not move, but process every part of the image in the same way. Local features are extracted at all locations and they are aggregated across different spatial regions in order to yield a representation of the whole image. Such a processing strategy has two major limitations. First, it is not scalable because the computational cost scales linearly with the number of pixels in the image. Since modern cameras take photographs that easily have more than 10M pixels, it would take several seconds if not minutes to analyze a single image. Second, the representation produced by such a system is *equivariant* as opposed to *invariant*, meaning that spatial translation and changes of scale are going to be reflected in the low level features that the system extracts. However, recognition tasks require the representation to be robust to such changes.

^{*}The author is currently with Facebook. This work was done while at Google.

Current state-of-the-art computer vision systems [2] have addressed these issues in several ways. First, images are often down-sampled to thumbnail size (typical resolution is 200 by 200 pixels, for instance). While this alleviates the scalability problem of searching over too many locations and scales [3], it seems a rather unsatisfactory solution because it limits recognition to objects that are at a rather coarse scale of the image. Second, invariance is achieved by computing histograms of local features over large regions at different locations and scales [4]. While this may achieve the desired outcome, it seems wasteful if not error prone to process regions of the image that do not contain the object of interest.

Today, the most computationally efficient and best performing methods employ the above mentioned strategies at their core. The best image recognition system, namely the Convolutional Neural Network [5, 2], is typically trained on small image patches and then "unrolled" over larger images at test time [6]. The key computation is the application of a sequence of stages, each composed by a non-linear filter bank across all spatial locations and scales, followed by some spatial pooling transform. Similarly, the best detection method, namely the Deformable Parts Model [7], applies a filter bank at all locations and scales, followed by a cascade of similar operations at the most promising locations in order to cut the computational cost [8].

In the past years, there have been several attempts at building a radically different paradigm of visual processing based on a foveated vision. However, most work in this area has been restricted to specific domains [9], to rather artificial tasks [10] and it has not been competitive on standard benchmark datasets [11].

In this work, we propose a method to learn where to look sequentially in images. The key idea is to first aggressively down-sample the image to cheaply detect candidate locations where to look at higher resolution. At test time, the information about low level features as well as the class distribution produced by this system are used to predict the location where to look next at high resolution. Given this location, a patch is cropped at the predicted location and it is fed to another system that predicts a new distribution over the classes. This process repeats for as many glimpses as necessary to reduce the uncertainty about the category of the object in the image. Information across the glimpses is integrated by taking a geometric mean of the intermediate predictions. At training time, the location of the glimpse is treated as a latent variable. Given a prediction of the location, we perturb this estimate and perform a local discrete search to find a better location.

Our empirical validation shows that this approach is able to achieve very competitive results on variants of the MNIST dataset [12] of handwritten digits. These experiments show that we can drastically cut the computational cost of classification while maintaining or even improving accuracy. The system does not waste computation in parts of the image that are unlikely to contain informative features and it does not waste computation on inputs that are simple enough to be classified confidently with few glimpses.

2 Algorithm

In this section, we will discuss how the system works at test and training time. In the next section instead, we will discuss how this relates to other methods.

2.1 Inference

Given an input image $X \in R^{D \times D}$, we want to predict its class label $y \in [0, 1, \dots, C]$. Notice that D may be large and therefore densely processing the whole image may be too expensive. In this work, we are going to consider multi-layer fully connected neural networks as classification methods. However, notice that this approach can be used with any other classifier as well.

The first step is to aggressively down-sample the image to a much lower resolution: $\bar{X} \in R^{d \times d}$ with $d \ll D$. Then, \bar{X} is fed to a fully connected neural network. Such network can have as many hidden layers as needed. For simplicity, here we assume that the network has only one hidden layer.

The transformations produced by this network are:

$$\mathbf{h}^{L} = \max(0, W_1^L \bar{X} + \mathbf{b}_1^L)$$

$$\mathbf{o}^{L} = W_2^L \mathbf{h}^L + \mathbf{b}_2^L$$
(1)

where W_1^L and W_2^L are weight matrices and \mathbf{b}_1^L and \mathbf{b}_2^L are biases. These are also the parameters that are subject to learning at training time. The output of the network, \mathbf{o}^L , is a C dimensional vector. By passing this vector through a softmax non-linearity we produce a distribution over the classes:

$$\mathbf{y}_k^L = \operatorname{softmax}(\mathbf{o}_k^L) = \frac{\exp(\mathbf{o}_k^L)}{\sum_j \exp(\mathbf{o}_j^L)}$$
 (2)

since each component of this vector is positive and components sum to one. We call this network the "low-resolution network" (N0), since it processes a down-sampled version of the original image. Next, the low level features \mathbf{h}^L and the output of the network \mathbf{o}^L are fed to another neural network that predicts the (normalized) (\mathbf{x},\mathbf{y}) coordinates of where to look next at high resolution. For simplicity but without loss of generality, here we consider a simple sigmoid layer:

$$\mathbf{l}^{p_1} = \sigma(W_1^{p_1} \mathbf{h}^L + W_2^{p_1} \mathbf{o}^L + \mathbf{b}^{p_1})$$
 (3)

where $\sigma(x)=1/(1+\exp(-x))$. Again, $W_1^{p_1}$, $W_2^{p_1}$ and \mathbf{b}^{p_1} are parameters which are subject to learning at training time. The predicted location, \mathbf{l}^{p_1} is a vector with two components between 0 and 1, specifying the (normalized) coordinates of the location where to look next at high resolution. More generally, we could also predict the width and the height of the patch as well as other properties.

At the next step, we crop a patch at the location specified by I^{p_1} from the high resolution image X, we denote this by $X(I^{p_1}) \in R^{w \times w}$. In this work, the patch is square and its diameter is fixed in advance to w.

We then feed the patch $X(\mathbf{l}^{p_1})$ to another neural network. Again, for the sake of simplicity we will refer to a one hidden layer neural network here. This network, which we call the first "glimpse network" (N1), computes:

$$\mathbf{h}^{H_1} = \max(0, W_1^{H_1} X(\mathbf{l}^{p_1}) + \mathbf{b}_1^{H_1})$$

$$\mathbf{o}^{H_1} = W_2^{H_1} \mathbf{h}^{H_1} + \mathbf{b}_2^{H_1}.$$
(4)

The resulting distribution over the class labels is given by the geometric mean between the output of the low-resolution network and the output of the first glimpse network:

$$\mathbf{y}^{H_1} = \operatorname{softmax}(\mathbf{o}^L + \mathbf{o}^{H_1}) \tag{5}$$

A schematic outline of the system is shown in fig. 1.

More generally, at the n-th glimpse the predicted class distribution is defined as:

$$\mathbf{y}^{H_n} = \operatorname{softmax}(\mathbf{o}^L + 1/n \sum_{j=1}^n \mathbf{o}^{H_j}). \tag{6}$$

where:

$$\mathbf{h}^{H_n} = \max(0, W_1^{H_n} X(\mathbf{l}^{p_n}) + \mathbf{b}_1^{H_n})$$

$$\mathbf{o}^{H_n} = W_2^{H_1} \mathbf{h}^{H_n} + \mathbf{b}_2^{H_n}.$$
(7)

Preliminary experiments showed that the choice of the weighting of the terms in the sum is not very important. This weighting yielded the best results but uniform weighting worked comparably well. The prediction of the location produced by the n-th glimpse network is:

$$\mathbf{l}^{p_n} = \sigma(W_1^{p_n} \mathbf{h}^L + W_2^{p_n} (\mathbf{o}^L + \sum_{j=1}^n \mathbf{o}^{H_j}) + \mathbf{b}^{p_n})$$
(8)

Note that $W_1^{H_n}$, $W_2^{H_n}$, $\mathbf{b}_1^{H_n}$, $\mathbf{b}_2^{H_n}$, $W_1^{p_n}$, $W_2^{p_n}$ and \mathbf{b}^{p_n} are parameters of the n-th glimpse network (Nn) which are subject to learning at training time.

These equations can be interpreted as follows. The system aggregates its predictions by taking a geometric mean of the class predictions at each glimpse (weighting more the prediction of the low resolution network). Taking a geometric mean amounts to multiplying probability estimates: the overall score is high only when several predictors agree about the presence of the object (akin to an "and" operation). The location is predicted by taking into account both low level features and the current prediction of the (un-normalized) class distribution. In our preliminary experiments, this configuration yielded the best results. However, the system is fairly robust to the kind of average used to integrate information across the glimpses as well as to the details of how predictions are computed (for instance, on MNIST the error rate increases by only 0.1% when using \mathbf{y}^{H_j} instead of \mathbf{o}^{H_j} for the prediction of where to look next).

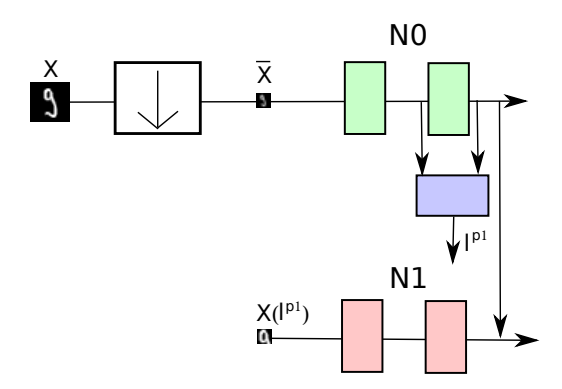


Figure 1: Outline of the model at inference time (showing only the first glimpse). The green blocks refer to the low resolution network, the purple block is used to predict the location where to look next and the red blocks represent the first glimpse network (taking as input the patch centered at the predicted location). The patch shown in the figure was predicted by a model trained on MNIST.

2.2 Learning

Since we are given a dataset that does not have target values for the locations where to look, it is going to be challenging to design an algorithm that can back-propagate through the cropping operator, because this operator is not differentiable. In this section, we are going to describe our solution to this problem in an incremental way.

First, we restrict ourselves to the problem of predicting the first location only and we observe that the location of where to look next can be interpreted as a latent variable, a variable upon which the loss depends but that it is not observed.

For each training sample X, we define the loss function as a compound sum of terms:

$$\mathcal{L}(\theta_0, \theta_1; X, \mathbf{z}, y^*) = E_0(\bar{X}, y^*; \theta_0) + E_1(X(\mathbf{z}), y^*; \theta_1) + \frac{\lambda}{2} ||\mathbf{l}^{p_1} - \mathbf{z}||^2$$
(9)

where θ_0 collectively denotes the parameters of the low resolution network $\{W_1^L, W_2^L, \mathbf{b}_1^L, \mathbf{b}_2^L, W_1^{p_1}, W_2^{p_1}, \mathbf{b}^{p_1}\}$, similarly θ_1 denotes the parameters of the first glimpse network $\{W_1^H, W_2^H, \mathbf{b}_1^H, \mathbf{b}_2^H\}$, $X(\mathbf{z})$ is the high resolution patch extracted at location \mathbf{z} , I^{p_1} is the predicted patch, X is a low resolution version of the input image X, y^* is the label of the input image and λ is a positive scalar.

The first term in the loss is the cross-entropy error of the low resolution network N0; if the correct class is k, then:

$$E_0(\bar{X}, y^k; \theta_0) = -\log(\mathbf{y}_k^L) \tag{10}$$

where \mathbf{y}_k^L is the probability assigned to the k-th class by the low resolution network (see eq. 2). Similarly, the second term in the loss is the cross entropy error of the first glimpse network (using eq. 5 as prediction of the output class). Finally, the last term measures the discrepancy between the location \mathbf{z} and the predicted one \mathbf{l}^{p_1} .

Similarly to generalized EM and to the Predictive Sparse Decomposition algorithm [13], we train by alternating between two steps. In the first step (the E step) we minimize the loss over the latent variables ¹:

$$\mathbf{z}^* = \arg\min_{\mathbf{z}} \mathcal{L}(\theta_0, \theta_1; X, \mathbf{z}, y^*)$$
(11)

This is the location which increases the log probability of the correct class while being as close as possible to the current prediction of the model. Since the cropping operation is not differentiable, we

¹In a probabilistic setting, this corresponds to computing a MAP estimate of the latent variables.

perform the minimization by a *local perturbation*: given the prediction of the model, we evaluate the loss at nearby image locations. In practice, we define a grid of points around the initial prediction (for instance, a 3 by 3 grid centered at the predicted location with points in the grid stepped every two pixels):

$$\mathbf{z}^* = \arg\min_{\mathbf{z} \in N(\mathbb{P}^1)} \mathcal{L}(\theta_0, \theta_1; X, \mathbf{z}, y^*)$$
(12)

where $N(\mathbf{l}^{p_1})$ is the discrete set of locations.

In the other step we minimize (or actually do a single step of gradient descent) over the parameters of the model fixing the latent variables to the value found at the previous step:

$$\theta_0 \leftarrow \theta_0 - \eta \frac{\partial \mathcal{L}(\theta_0, \theta_1; X, \mathbf{z}^*, y^*)}{\partial \theta_0}$$
(13)

$$\theta_1 \leftarrow \theta_1 - \eta \frac{\partial \mathcal{L}(\theta_0, \theta_1; X, \mathbf{z}^*, y^*)}{\partial \theta_1}$$
 (14)

where η is a scalar learning rate. After this gradient step, the network will produce a better prediction of the location where to look next and it will increase the log probability of the correct class.

The minimization over the location variables seems rather wasteful since only the location yielding the lowest loss is retained. We have found empirically (see sec. 4.1.1) that accuracy considerably improves by considering also the "most offending" location [14], that is the location where the network is most confident about a class that is incorrect:

$$\mathbf{z}^{-} = \arg\min_{\mathbf{z} \in N(\mathbf{l}^{p_1}), y \neq y^*} \mathcal{L}(\theta_0, \theta_1; X, \mathbf{z}, y)$$
(15)

We can now add another term to the loss function which is the cross-entropy at location z^- ; after the minimization we have:

$$\mathcal{L}(\theta_0, \theta_1; X, y^*) = E_0(\bar{X}, y^*; \theta_0) + E_1(X(\mathbf{z}^*), y^*; \theta_1) + E_1(X(\mathbf{z}^-), y^*; \theta_1) + \frac{\lambda}{2} ||\mathbf{l}^{p_1} - \mathbf{z}^*||^2$$
(16)

This forces the system to increase the probability of the correct class at the most confusing location as well. This improves generalization because the location predictor may not be very accurate (overall if λ is small) and this makes the system predict the correct class not only at the best location but also at nearby ones.

2.2.1 Extension to Multiple Glimpses

For the sake of simplicity, we propose to train each glimpse in sequence. Once, the first glimpse is trained using the algorithm described above, we train the second glimpse network while holding fix the parameters of the low resolution network as well as the parameters of the first glimpse network. More generally, given the first k-1 glimpses we train the k-th glimpse network holding fix all the other parameters. This greedy algorithm is very simple and worked well in our experiments.

The learning algorithm is the same as the one described above, alternating between a step which makes a discrete search over locations, and a step which makes a gradient step over the parameters.

The location is predicted using eq. 8 while the output of the glimpse network is given by eq. 7. Since we fix the parameters of the first k-1 glimpse networks, the loss reduces to:

$$\mathcal{L}(\theta_k; X, y^*) = E_k(X(\mathbf{z}^*), y^*; \theta_k) + E_k(X(\mathbf{z}^-), y^*; \theta_k) + \frac{\lambda}{2} ||\mathbf{l}^{p_k} - \mathbf{z}^*||^2$$
(17)

In our preliminary experiments, we have found that on certain datasets classification accuracy slightly improves when we constrain the location of each glimpse to be far away from the locations of previous glimpses. In order to achieve this, we add to the loss function a penalty for making predictions that are too close to each other using the following term:

$$\gamma \sum_{j=1}^{k-1} e^{-\frac{1}{2} \frac{||\mathbf{z} - \mathbf{l}^{p_j}||^2}{\sigma^2}} \tag{18}$$

This effectively puts a Gaussian bump penalty around each previously visited position, encouraging the new prediction to be in a different position.

2.2.2 Fine Tuning

Since the prediction is never optimal (i.e., yielding the minimum of the loss function) unless λ is very large, in the last stage of training we set the location to the predicted value (effectively setting λ to infinity) and update only the parameters. This tunes the parameters to fit the actual prediction that will be used at test time.

2.2.3 Other Extensions

There are several other extensions to the baseline model:

- using multi-scale inputs when extracting high-resolution patches in order to cheaply leverage larger context (akin to a crude approximation of the log-polar resolution of the fovea [15, 11]),
- using gating interactions to modulate the features extracted by the glimpse network to take into account also the location where the patch was extracted,
- using gating interactions to predict the location (as opposed to doing a simple weighted sum),
- \bullet predicting at every step M locations in parallel as opposed to only one,
- as training proceeds, reducing the grid size used for searching over locations.

In sec. 4 we will evaluate some of these extensions.

2.2.4 Summary

To summarize, training proceeds by:

- 1. train N0 and N1
- 2. train N2, fixing N0 and N1
- 3. train N3, fixing N0, N1 and N2
- 4. etc.
- 5. fine-tune: using the predicted location, adjust the parameters of the last glimpse network to minimize the loss.

The training of each glimpse is done by stochastic gradient descent with momentum set to 0.9. For each training sample, we alternate between:

- finding the location that yields the lowest loss as well as the location that yields the most confident but wrong prediction (see eq.11 and 15).
- updating the parameters by one step of gradient descent using the loss in eq. 17.

3 Relation to Other Models

In this section, we relate the proposed method to some prior work. First, there has been a lot of work on methods that produce saliency maps [16, 17]. Although these works share the same aim, that is to cut the computational cost of analyzing very large images by focusing on the most informative regions, they compute such maps in a task-independent manner and they typically rely on heuristics [18].

The proposed method is certainly related to the work by Larochelle and Hinton [11]. Both methods learn all parameters and they are task driven. Both methods aggregate information across glimpses by using the geometric mean of the predictions across glimpses. However, our method is trained in a fully discriminative manner using a rather different loss and optimization method. Also, we do not overlay a grid over all possible locations in the image but use local perturbations which can be computed more efficiently.

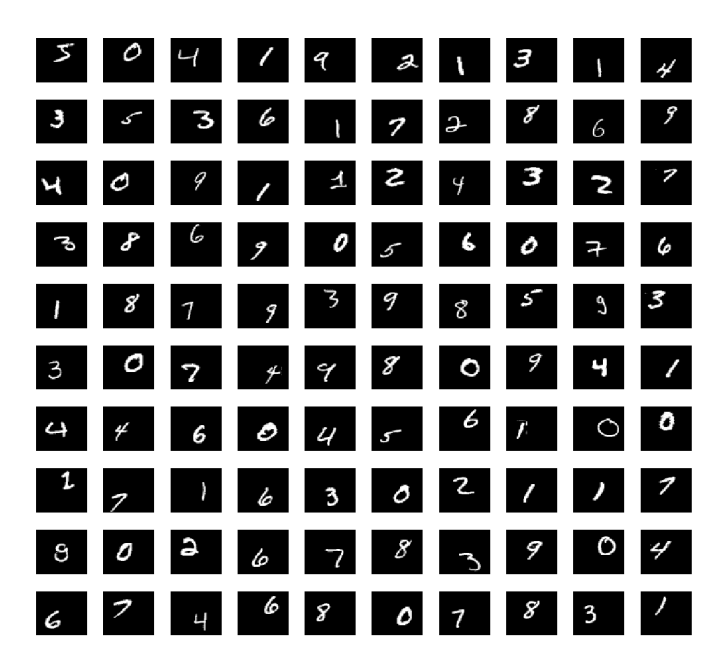


Figure 2: Examples of images in the jittered MNIST dataset. Each image has size 48 by 48 pixels and digits are placed at random locations in the image.

The particular learning algorithm we chose was inspired by the Predictive Sparse Decomposition (PSD) algorithm [13]. Similarly to this sparse coding algorithm, training alternates between two steps. In the first step we find the most likely state of some latent variables (in PSD these are the sparse codes while in this work these are variables encoding the spatial position of where to look next at high resolution). Notice however that the optimization technique we employ is drastically different: in this work we minimize by a local discrete perturbation because the objective is not differentiable, while in that work they minimize by gradient descent. Also, in this work the loss includes a contrastive term which is absent in PSD. In the second step, the parameters are updated by gradient descent in both algorithms. Although the design of the loss function may resemble the one proposed here, the task and the meaning of the variables is very different: in [13] the objective is reconstructing the input while here the objective is to classify, in [13] the variables represent internal features while here they represent spatial locations.

If the glimpse networks share the same parameters (except for the module that predicts the location) and we augment the model with gating units that make the hidden units depend on the selected location, then the proposed method is also related to Recurrent Neural Networks (RNN). The major difference is that in this model the input which is fed to the system is self-determined at each step, as opposed to be provided by the user.

Finally, the proposed method can also be related to cascade approaches and boosting [8]. As we shall see in the next section, it is possible to set a threshold on the confidence of the classifiers and use that to make an amount of computation which depends on the complexity of the input. In fact, most input images exhibit patterns that are simple enough to be classified well by the low resolution network itself. Fewer and more complex patterns instead require the processing of the subsequent glimpse networks. This approach which is reminiscent of cascading, makes classification very fast and adaptive to the complexity of the input, as we shall see in sec. 4.1.

4 Experiments

Most of our experiments are reported on a variant of the MNIST dataset [12]: the jittered MNIST dataset. This dataset consists of 48 by 48 pixel images that were constructed by placing at a random location the original 28 by 28 pixel image and by filling with zeros the remaining pixel values. A random subset of the images in this dataset is shown in fig. 2. The training set consists of 600,000 images (each image from the original MNIST training set generates 10 images with the same digit at different random locations) and 30,000 images in the test set.

The advantage of this dataset is that the system is less prone to overfit and therefore, we can better assess the quality of different training strategies without worrying too much about the confounding factor of regularization.

For the sake of comparison, we also report experiments on the original MNIST dataset. These experiments demonstrate that the proposed method perform as well or very close to convolutional networks (which are the state-of-the-art classification method on this dataset), while being several times more computationally efficient.

4.1 Jittered MNIST

In this experiment, the input images have size 48 by 48 pixels. These are down-sampled to 12 by 12 pixels before being fed to the low resolution network N0. The high resolution patches have also size 12 by 12 pixels and we consider two scales: the original one and half of the original one. In other words, the glimpse networks take as input two patches of size 12 by 12 pixels, where the second patch is actually a down-sampled version of a 24 by 24 patch.

During training, the search over spatial locations is performed over a 3 by 3 grid of points that are spaced every 2 pixels (as measured at the finest resolution). We tried other patch sizes, grid sizes, etc. and we found that the performance is fairly robust to the choice of these hyper-parameters. In all our experiments we set λ to 100, γ to 0.01 and σ^2 to 0.002 (see eq. 17 and 18). Finally, during training we run for 50 sweeps over the training set using stochastic gradient descent on mini-batches of size 50 with momentum set to 0.9 and learning rate set to 0.05.

Tab. 1 reports the results in terms of error rate and speed up with respect to the number of flops required by a fully connected network trained on the original 48 by 48 images. All networks we consider (N0, N1, N2 as well as the fully connected baseline) have one hidden layer with 500 hidden units. We also compare to a convolutional network which is the best classification system on this data. The convolutional network has two stages of convolution and max-pooling, each of which with 64 filters of size 5 by 5 and with pooling neighborhood of 2 by 2 pixels stepped every 2 pixels. These two stages are followed by a fully connected layer with 128 hidden units and by a top layer with 10 units, as many as the classes we want to predict.

We found that adding glimpses helps performance (a third glimpse yielded only marginal improvements though). Moreover, fine-tuning (as described in sec. 2.2.2) further reduces the error rate and makes the system match the performance of the convolutional network. Notice however that the amount of computation required by our method is 2 order of magnitude lower than what is required by a convolutional network.

Table 1: Results on the jittered MNIST dataset. A speed-up equal to 12 means that the corresponding method makes 12 times less flops than the baseline fully connected network operating on the original high resolution images.

Method	Test Error Rate%	Speed-Up
fully connected on high resolution images	3.5	1.0
convolutional network	1.4	0.03
this method, 1 glimpse	2.3	5
this method, 2 glimpses	1.6	3
this method, 2 glimpses, fine tuned	1.4	3
this method, 2 glimpses, cascaded	1.7	12

The last row of tab. 1 shows the performance of our system when using a threshold on the confidence of the prediction in order to further cut the computational cost. By setting a threshold of 0.95 on the output of the classifiers, we have that 78% of the test samples can be classified by just the low resolution network. Among the classified samples, we have have an error rate of 0.45% and an overall rejection rate of 22%. The first glimpse network classifies 15% of the digits (relative to the total number of test samples) and the second glimpse network 3% of the digits with a final rejection rate of 4.8%. If we let N2 classify all digits regardless of its confidence, the overall test error rate becomes 1.7%, only 0.1% worse than the reference model (which runs all samples through all the networks N0, N1 and N2). Since most samples are confidently classified by N0, the computational saving is very large: 12 times more efficient than using the fully connected baseline.

4.1.1 Control Experiments

In this section, we further investigate the proposed model teasing apart the contribution of each component of the system. The experimental set up is the same as the one described in the previous section. In the first experiment, we validated the effectiveness of the use of multi-scale inputs in N1. As the first two rows of tab. 2 show, the test error rate is greatly reduced by providing the network with more context. We conjecture that this makes the network also more robust to errors in the exact prediction of the location where to look next.

In the next experiment we remove the contrastive term in the loss function which measures the cross entropy at the most offending location (see third term on the right hand side of eq. 16). This dramatically increases the error rate, demonstrating that it is very important to lower the score of incorrect labels at nearby locations.

In the fourth and fifth row of tab. 2 we report the error rate when the two glimpses are performed sequentially and in parallel. In the latter experiment, the prediction of the location of the first and second glimpses takes the same input, namely the first hidden layer and the output of N0. This experiment aims at assessing the importance of the sequential nature of the inference process we proposed. The error rate does increase but not very much, suggesting that the greedy algorithm we proposed is better but we would not compromise too much accuracy by performing predictions in parallel. This suggests that we may reach a better trade-off between computational efficiency and accuracy by performing M sequential predictions, each composed by K parallel glimpses. We leave further exploration of this conjecture to future investigation.

In the next experiment, we verify the effectiveness of the error term penalizing predictions of nearby locations (see eq. 18). By removing this term the error rate actually decreases by 0.2%, suggesting that this term could be safely removed from the loss 2 . If we fine tune the last glimpse network using this set up, we reach an error rate of 1.2%, which is the lowest error rate we could report on this dataset

Finally, we report the error rate when the parameters in N1 and N2 are tied to each other. The last row of tab. 2 shows that using the same parameters for different glimpses increases the error rate by only 0.1%.

Table 2: Control experiments on the jittered MNIST dataset.

Method	Test Error Rate%	Speed-Up
this method, 1 glimpse (multi-resolution)	2.3	5
this method, 1 glimpse (single resolution)	4.2	7
this method, 1 glimpse (single resolution), no contrastive term	14.0	7
this method, 2 glimpses	1.6	3
this method, 2 glimpses, done in parallel	1.75	3
this method, 2 glimpses, no diversity penalty	1.4	3
this method, 2 glimpses, no diversity penalty with fine tuning	1.2	3
this method, 2 glimpses, with weight sharing	1.7	3

²However, on the original MNIST dataset the error rate increases by 0.1% when removing this term.

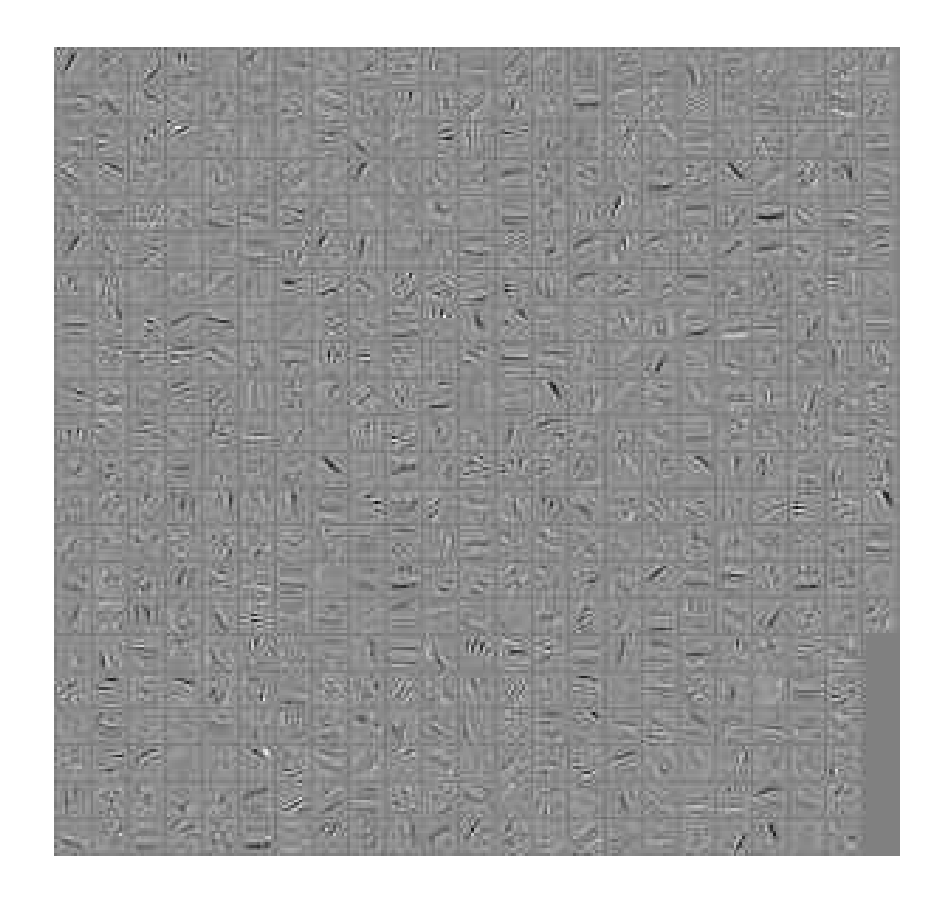


Figure 3: Each tile is a filter learned by the low resolution network N0.

4.1.2 Visualizations

In this section, we provide qualitative intuitions as to what the system is doing. Fig. 3 and 4 show the filters (i.e., weights connecting each hidden unit to the corresponding input) learned by N0 and N1. All filters seem to be used and they converge to highly tuned stroke detectors. We conjecture that the network performs its classification by doing a global pattern matching using the low resolution images, and a highly tuned local feature matching using N1 and N2.

In fig. 5 we show examples were the predictions produced by N0, N1 and N2 differ the most. First, we observe that N1 and N2 look at different locations in order to disambiguate the low resolution image (for instance, N1 looks at the top part of 3 and 8 while N2 looks at the bottom part of these images). Second, the prediction is often refined as glimpses are added and evidence aggregated. And finally, the predicted location tracks well the digit as it moves in the canvas.

4.2 MNIST

In the last experiment, we report experiments on the original version of the MNIST dataset in order to compare to previously published results [12]. In this experiment, the input images have size 28 by 28 pixels while the down-sampled images have size 10 by 10 pixels. The size of the patches that we crop from the high resolution images is also 10 by 10. Given the small size of the original images in this dataset, we report results using only a single resolution (the finest). During training the search over locations is performed by considering a 3 by 3 grid of points strided every 2 pixels. Finally, during training we run for 50 sweeps over the whole training set using stochastic gradient descent on mini-batches of size 50 with momentum set to 0.9 and learning rate set to 0.01.

Tab. 3 compares our method to standard baselines (fully connected network taking the original and the down-sampled input as well as a convolutional network). We also compare to our method with a fixed glimpse at the center of the image (since the MNIST digits are registered, the central

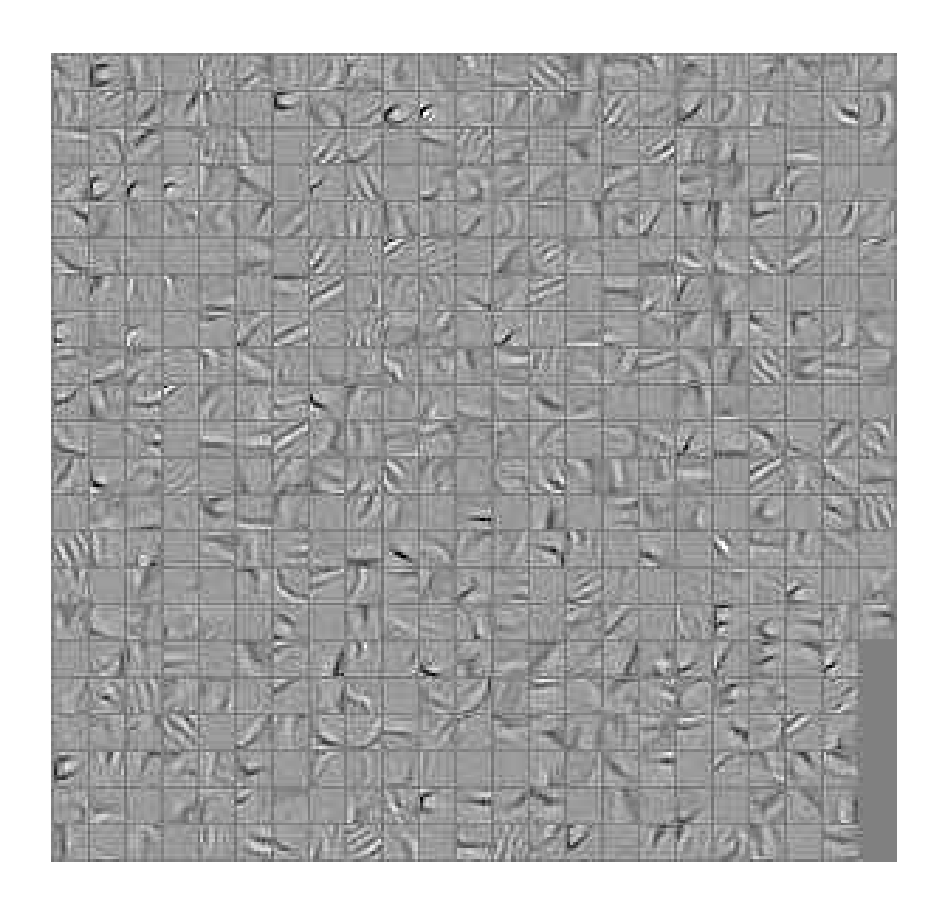


Figure 4: Each tile is a filter learned by the first glimpse network N1 (applied to high resolution patches).

patch is the most informative one). We observe that our method generalizes better than a fully connected network, and it approaches the performance of a convolutional network (without adding any regularization) when we learn where to look in the image. A second glimpse produced only marginal gains (a reduction of 0.1% test error rate) due to severe overfitting.

Table 3: Results on MNIST dataset; the speed-up is relative to the fully connected network. Original images have size 28 by 28 pixels, down-sampled images have size 10 by 10 pixels, high resolution patches have size 10 by 10 pixels. Notice that the reported results of [11] was achieved by training on 10,000 training samples only. Our method achieves the same accuracy when trained on such a small subset of the training data. According to Larochelle, their method [11] does not scale easily to the full size of the dataset.

Method	Test Error Rate%	Speed-Up
fully connected on high resolution images	1.8	1.0
fully connected on down-sampled images	7.7	7.2
this method, 1 glimpse fixed at the center of the image	2.0	3.6
convolutional network	0.8	0.05
prior work [11]	2.7	N/A
this method, 1 glimpse	1.2	3.6

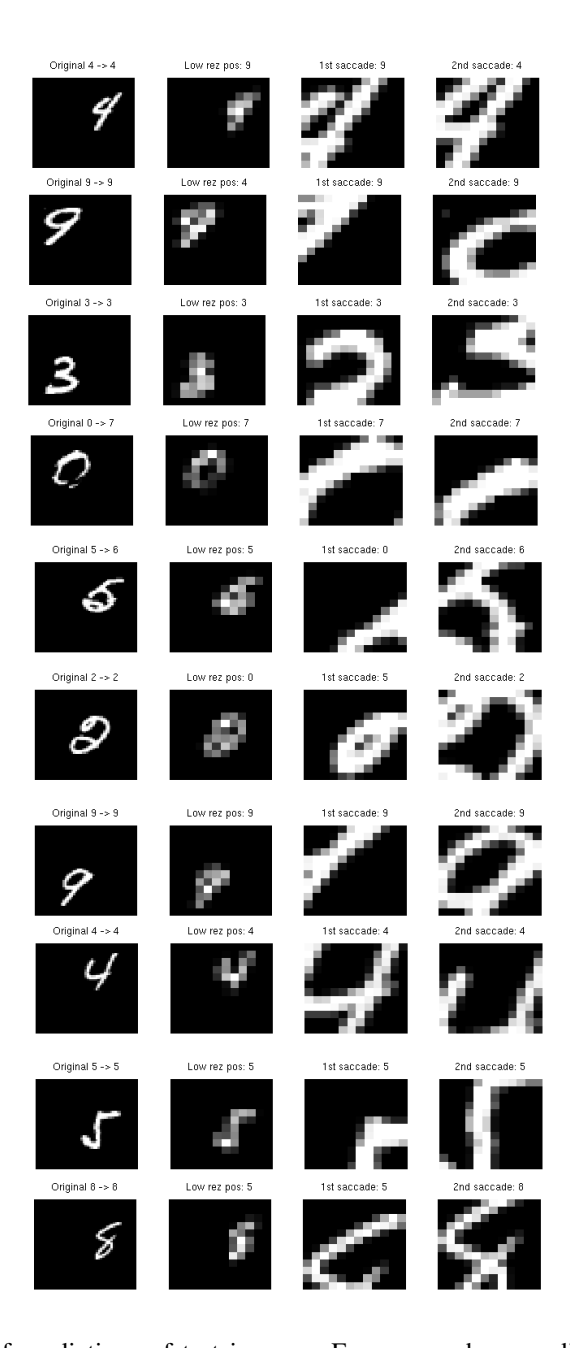


Figure 5: Examples of predictions of test images. Every row shows a different example. The columns show (from left to right): the original image X (with the correct class label and the predicted class label), the down-sampled image \bar{X} of size 12 by 12 pixels (with the predicted class produced by N0 network), the high resolution patch used by the first glimpse network N1 (with the its class prediction) and the high resolution patch fed to the second glimpse network N2 (with the corresponding class label prediction). Note that each image has been resize to fit the grid, but the images in the first column have size 48 by 48, while the images in the other columns have size 12 by 12 pixels.

5 Conclusions

In this work, we introduced a new model to classify images through a sequence of glimpses. The whole system is trained in a discriminative manner by alternating between two steps. In the first step, we find the best locations where to look next as measured by the increase in the likelihood of

the image belonging to the correct class. In the second step, the parameters of the model are updated in order to improve both prediction of where to look next as well as prediction of the object category.

After training, the model is computationally very efficient since a simple forward pass yields the class prediction. Moreover, the sequential processing of the method can be leveraged to further cut its computational cost: the next glimpse is used only when the current prediction has low confidence. We have shown that such a method perform comparably well to state-of-the-art classification methods at a tiny fraction of their computational cost.

Future work will investigate the use of this method on more challenging benchmarks for both classification and detection.

6 Acknowledgements

I would like to thank Geoff Hinton for encouraging me to work on this project and for his advises. I would like to thank also Ilya Sutskever and Jay Yagnik for very helpful discussions and suggestions, and Andrew Senior and Alex Krizhevsky for their help in running experiments on GPU. Finally, this project could not have been accomplished without the support from Jeff Dean and the Google Brain team at Google.

References

- [1] P.J. Erichsen and J.M. Woodhouse. Human and animal vision. *Machine Vision Handbook*, 2013.
- [2] A. Krizhevsky, I. Sutskever, and G. E. Hinton. Imagenet classification with deep convolutional neural networks. In *NIPS*, 2012.
- [3] H. Rowley, S. Baluja, and T. Kanade. Neural network based face detection. *IEEE Transactions on Pattern Analysis and Machine Intelligence*, 1998.
- [4] S. Lazebnik, C. Schmid, and J. Ponce. Beyond bags of features: Spatial pyramid matching for recognizing natural scene categories. In *IEEE Conference on Computer Vision and Pattern Recognition*, June 2006.
- [5] Y. LeCun, L. Bottou, Y. Bengio, and P. Haffner. Gradient-based learning applied to document recognition. *Proceedings of the IEEE*, 86(11):2278–2324, 1998.
- [6] M. Osadchy, Y. LeCun, and M. Miller. Synergistic face detection and pose estimation with energy-based models, 2007.
- [7] P. Felzenszwalb, R. Girshick, and D. McAllester. Cascade object detection with deformable part models. In *IEEE Conference on Computer Vision and Pattern Recognition*, 2010.
- [8] P. Viola and M. Jones. Rapid object detection using a boosted cascade of simple features. In *IEEE Conference on Computer Vision and Pattern Recognition*, 2001.
- [9] J. Elder, S. Prince, Y. Hou, M Sizintsev, and E. Olevskiy. *Int. Journal of Computer Vision*, 72:4766, 2007.
- [10] L.W. Renninger, J. Coughlan, P. Verghese, and J. Malik. An information maximization model of eye movements. In *Advances in Neural Information Processing Systems*, 2005.
- [11] H. Larochelle and G.E. Hinton. Learning to combine foveal glimpses with a third-order boltzmann machine. In *Advances in Neural Information Processing Systems*, 2010.
- [12] http://yann.lecun.com/exdb/mnist/.
- [13] K. Kavukcuoglu, M. Ranzato, and Y. LeCun. Fast inference in sparse coding algorithms with applications to object recognition. Technical report, Computational and Biological Learning Lab, Courant Institute, NYU, 2008. Tech Report CBLL-TR-2008-12-01.
- [14] Y. LeCun, S. Chopra, R. Hadsell, M. Ranzato, and F.J. Huang. A tutorial on energy-based learning. *Predicting Structured Data*, 2006.
- [15] J. Freeman and E.P. Simoncelli. Metamers of the ventral stream. *Nature Neuroscience*, 14(9):1195–1201, 2011.

- [16] L. Itti, C. Koch, and E. Niebur. A model of saliency-based visual attention for rapid scene analysis. *IEEE Trans. Pattern Analysis and Machine Intelligence*, 20(11):1254–1259, 1998.
- [17] C. Kanan and G. Cottrell. Robust classification of objects, faces and flowers using natural image statistics. In *IEEE Computer Vision and Pattern Recognition*, 2010.
- [18] S. Goferman, L. Zelnik-Manor, and A. Tal. Context-aware saliency detection. *IEEE Trans. on Pattern Analysis and Machine Intelligence*, 34(10):1915–1926, 2012.